Research Article

Treatment of Marigold Flower Processing Wastewater Using a Sequential Biological-Electrochemical Process

Lokesh Kumar Akula, Raj Kumar Oruganti and Debraj Bhattacharyya*
Department of Civil Engineering, Indian Institute of Technology Hyderabad, Telangana, India

Kiran Kumar Kurilla
Kaashyap Envergy Infrastructures Pvt. Ltd., Telangana, India

* Corresponding author. E-mail: debrajb@ce.iith.ac.in DOI: 10.14416/j.asep.2021.04.001
Received: 19 November 2020; Revised: 12 January 2021; Accepted: 19 February 2021; Published online: 19 April 2021

Abstract
Agriculture is the mainstay of the Indian economy. The agro-based industries produce high volumes of high-strength wastewaters that need to be treated and reused to prevent environmental pollution and water wastage. This study evaluated the performances of a sequential biological-electrochemical process for treating an anaerobically digested effluent of a Marigold flower processing agro-industry. The uniqueness of this wastewater possess a major challenge to its treatment since not many studies have been conducted on this wastewater. The biological treatment was carried out in a Sequential Batch Reactor (SBR). The treated water was further polished in a Continuous Bipolar-mode Electrochemical Reactor (ECR) to remove the residual organics. The anaerobically digested effluent Chemical Oxygen Demand (COD), Dissolved Organic Carbon (DOC), Total Nitrogen (TN), Total Phosphorus (TP) and Total Suspended Solids (TSS) were 5750 ± 991 mg/L, 980 ± 120 mg/L, 692 ± 60 mg/L, 9.7 ± 1.1 mg/L, and 1144 ± 166 mg/L, respectively. A significant level of treatment was achieved in the SBR. The combined system was able to remove 79% of COD, 85% of DOC, 53% of TN, and almost 100% of TP, TSS, and Volatile Suspended Solids (VSS). Several organic compounds belonging to the category of natural plants compound, pesticide, fungicide, etc. were detected in the raw wastewater. Most of the compounds were almost completely removed by the treatment system. The final effluent was almost colorless and free from suspended solids. However, for reuse, the water needs to be further treated in an advanced oxidation process.

Keywords: Electrocoagulation, Marigold flower processing wastewater, Sequential Batch Reactor, Wastewater treatment

1 Introduction

The global trends in industrialization and urbanization have imposed a high burden on the environment, including freshwater resources. In many parts of the world, especially in agrarian countries like India, rapid development in agro-based industries poses a danger to water quality and creates stress on water supplies [1]. The 'State of Indian Agriculture report 2015–16' indicates that agriculture and related sectors will continue to play a vital role in the growth and development of the Indian economy [2]. The effluents from agro-based industries contain a high amount of organic matter and will cause environmental issues if disposed of untreated [3]. Generally, the agro-based industrial wastewaters are high in chemical and biological oxygen demand, solids, phosphorus, and nitrogen [4]. However, agro-based industrial effluents, being less

Please cite this article as: L. K. Akula, R. K. Oruganti, D. Bhattacharyya, and K. K. Kurilla, "Treatment of marigold flower processing wastewater using a sequential biological-electrochemical process," *Applied Science and Engineering Progress*, vol. 14, no. 3, pp. 525–542, Jul.–Sep. 2021, doi: 10.14416/j.asep.2021.04.001.

toxic (unlike those originating from pharmaceutical, textile, dye, and pesticide industries), can be reused if properly treated and renewable energy can be generated as a by-product [5].

Cultivation of commercial crops, like marigold flowers, comes under the floriculture sector, where farmers are currently getting excellent returns. Lutein, belonging to a group of plant pigments called xanthophylls, is found in abundance in marigold flowers and possesses anticancer and antioxidant properties [6]. Lutein is a bright orange-colored phytochemical that is extracted from marigold flower petals after fermentation using organic solvents. The 'Oleoresin Marigold' has applications not only in the pharma industry but also in the nutrition, dye, and pet food industries. Generally, the marigold flower contains 80–90% moisture during fermentation, which is released as effluent during the squeezing process. This wastewater has been identified as a major source of water pollution due to its high Chemical Oxygen Demand (COD) (50,000–60,000 mg/L) and Biochemical Oxygen Demand (BOD). Therefore, this effluent requires proper treatment before being disposed of or reused.

Anaerobic treatment is one of the important options for treating different types of industrial wastewaters [7]. Agro-based effluents, due to their high organic strength, are treated biologically in Upflow Anaerobic Filter process (UAF), Anaerobic Fluidized-Bed (AFB) Reactor, Upflow anaerobic Sludge Blanket (UASB), and facultative pond systems [4]. However, treatment of agro-wastewater in anaerobic treatment alone cannot treat effluents to a level that matches the discharge limit prescribed by regulatory bodies. Aerobic and/or physicochemical polishing of wastewater is required for meeting the discharge criteria.

A marigold flower processing plant in southern India has adopted anaerobic biological treatment for treating a highly concentrated effluent. Very few papers are available on the treatment of this type of wastewater [8]–[10]. The uniqueness of the wastewater presented a major challenge to its treatment. It was observed that the anaerobically digested effluent contained a significant amount of color and organics and, therefore, needed to be further treated to generate water for reusable purposes. The anaerobically digested Marigold Flower Wastewater (MWW) was amenable to aerobic treatment; thus, a sequenced anaerobic-aerobic treatment appeared to be a technically viable approach. In this study, the anaerobically-digested effluent was further treated aerobically. The aerobic treatment significantly removed the organics. However, it was observed that the treated wastewater still contained color and organic matter and, therefore, needed physicochemical polishing to remove the residual color and organics.

A modified aerobic Sequential Batch Reactor (SBR) was installed at the existing plant facility under this project to polish the anaerobically treated MWW. SBR operates in five sequential phases, namely, 'Fill', 'React', 'Settle', 'Draw' or 'Decant', and 'Idle' (during which withdrawal of excess sludge is also accomplished) [11]. SBR is known for its operational flexibility and better kinetics; therefore, it requires a lesser footprint. Moreover, only a single tank is required for equalization, aeration, and clarification, which results in considerable savings in capital cost. The SBR technology has been successfully implemented in the past for treating palm oil mill effluent, tannery wastewater, Paper and Pulp Mill Effluent, and complex chemical wastewaters [12].

The biologically treated effluents usually contain residual recalcitrant organics and color and, therefore, require a physicochemical polishing treatment. The usual polishing treatment adopted at the industry-scale includes a reverse osmosis process followed by the multiple-effect evaporator and incineration that makes the process very energy-intensive. The Electrochemical (EC) process is gaining popularity among the physicochemical processes because of its low-cost material and simple process design [13]. With the advent of bipolar mode EC systems, the operating cost is also getting reduced significantly [14].

During an electrochemical process, a set of reactions and chemical phenomena occur, which includes - (a) the dissolution of metal ion from the anode, (b) oxidation of the metal ions, and the formation of metal complexes or coagulants which finally settle as flocs, and (c) evolution of gases at the electrodes due to electrolysis of water. The pollutants are removed from wastewater through (a) adsorption onto the surface of the coagulants, (b) chemical precipitation onto the sludge, and (c) passive oxidation at the electrode (in case of organic carbon). EC process has been successfully employed in removing suspended and dissolved solids, colloidal particles, metal ions, pesticides, pharmaceutical compounds [15], [16], radionuclides, and also harmful microorganisms [17] from wastewater. Some of the reactions that happen at the electrodes are as follows:

At Anode [Equations (1)–(2)]:

$$4Fe_{(S)} \rightarrow 4Fe^{2+}_{(aq)} + 8e^{-} \quad (1)$$

$$4Fe^{2+}_{(aq)} + 10H_2O + O_{2(g)} \rightarrow 4Fe(OH)_{3(S)} + 8H^{+} \quad (2)$$

At Cathode [Equation (3)]:

$$8H^{+} + 8e^{-} \rightarrow 4H_{2(g)} \quad (3)$$

Overall [Equation (4)]:

$$4Fe_{(S)} + 10H_2O + O_2 \rightarrow 4Fe(OH)_{3(S)} + 4H_{2(g)} \quad (4)$$

Besides, precipitation of dissolved pollutants also happens during the EC process [Equation (5)].

$$Fe^{3+} + PO_4^{3-} \leftrightarrow 4FePO_{4(S)} \quad (5)$$

A Continuous-flow Bipolar-mode Electrochemical Reactor (ECR) was used in this study. The ECR, which had a series of sacrificial electrodes inserted between the two end electrodes (which are connected to the power supply), required less footprint, reaction time, and energy compared to mono-polar mode electrochemical reactors for the same degree of wastewater treatment [9].

As mentioned in the beginning, the overall objective of this research work was to treat the effluent of a marigold flower processing (agro-based) industry and bring the quality of the treated water up to a reusable standard. The industry already has an existing treatment plant. The wastewater was collected from the existing anaerobic digester and pumped into the SBR, which was operated at different cycles. A part of the effluent from the SBR was directly pumped into the ECR when the SBR was operating at the lowest cycle time. The ECR was operated at different pH, reaction time, and current. Standard Design of Experiment (DoE) procedures Central Composite Design (CCD) and Response Surface Methodology (RSM)) were followed to model and optimize the EC treatment process. COD, Dissolved Organic Carbon (DOC), Total Phosphorus (TP), Total Nitrogen (TN), Total Suspended Solids (TSS), and Volatile suspended solids (VSS) were measured. Also, organic constituents of the wastewater were identified in the feed water and the treated effluent.

2 Materials and Methods

2.1 *Wastewater sampling*

The experimental work was carried out at Synthite Industries Pvt Ltd, located in a village called Teligi in the Davanagere district of the state of Karnataka in India. The raw wastewater was generated mainly from the Marigold flower squeezing unit. The untreated wastewater had a COD in the range of 50,000–60,000 mg/L, which was fed to an anaerobic reactor. In the anaerobic reactor, around 90% of COD was removed. The anaerobically digested effluent still had a significant amount of COD and was dark in color. This effluent was used in the present study.

2.2 *Experimental setup*

2.2.1 SBR Setup

The SBR used in this study was a 7000 L circular steel tank (Diameter = 2.25 m; Height = 2.25 m; Working volume = 4250 L). The reactor had several improved features, which include a compartmentalized sloping base, retractable diffusers that can be repaired easily, and other improved features aimed at simplifying the reactor operation (for example, wasting of sludge and retaining adequate biomass in the reactor) and regular maintenance. A floating decanter was used. The decanter had spring-based valves at the inlet that prevented the accumulation of suspended solids inside the decanter during the aeration phase. Consequently, the escape of suspended solids with the treated effluent was also minimized. The decanter was kept afloat near the surface of the water using a floating device, which enabled it to move up and down along with the water level in the SBR. This feature allowed the treated water to be decanted from the top, which, in turn, can reduce the overall cycle time since the 'Decant' phase of SBR can be started even before the 'Settle' phase is complete. A schematic of the reactor is shown in Figure 1(a). A Programmable Logic Controller – Motor Control Centre (PLC-MCC) (Siemens make) was used to control the sequence of the entire SBR operation. The organization of these devices followed a standard feedback control scheme. The PLC computer program automatically controlled pumping, aeration, settling, and discharge functions.

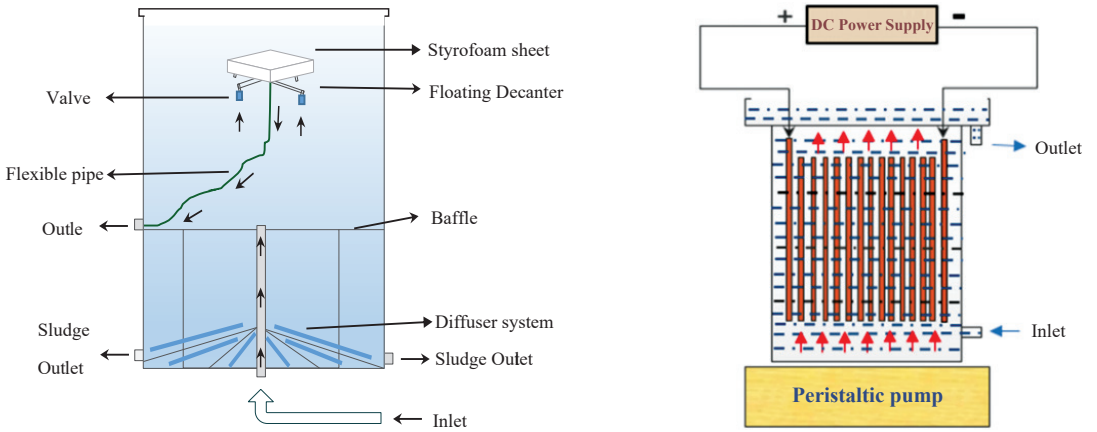

(a) (b)

Figure 1: Schematic representation of the reactors (a) SBR system (b) ECR system.

2.2.2 ECR setup

A 1-L Continuous-flow Bipolar-mode Electrochemical Reactor (ECR), having an effective volume of 765 mL, was connected in series with the SBR. A part of the SBR effluent was directly pumped into the ECR for treatment. The ECR was made up of polyacrylic sheets. A schematic representation of the experimental setup is shown in Figure 1(b). The reactor consisted of an array of 15 parallel MS electrodes (98% purity), each having dimensions 15 cm × 3.4 cm × 0.3 cm. The end electrodes were connected to DC (Direct Current) current supply with a variable output of 0–220 V. The central electrodes worked as sacrificial electrodes. After being treated in SBR, the MWW was fed to the ECR from the bottom. As the water rises through the inter-electrode spaces, the pollutants get mixed with the iron adsorbent, released from the anode, and are swept away along with the treated effluent from the top. Precipitation of some soluble substances also takes place in the reactor. Precipitates also leave the system from the top along with the effluent. The precipitate and the pollutant-laden iron adsorbent are separated from the treated wastewater in a clarifier. A part of the organic carbon may get oxidized to carbon dioxide at the electrode while a part of nitrogen may escape in the form of ammonia and gaseous nitrogen.

2.3 *Experimental procedure*

The experiment was divided into two phases. The flow diagram of the experimental procedure is shown in Figure 2. The phase-1 experiment was carried out only with the SBR, and in phase-2, an ECR unit was used in series when the SBR was operated at the lowest cycle time. The performance evaluation was carried out for both the phases based on COD, DOC, TN, TP, and TSS removals. The effluent was also analyzed for organic constituents and pathogens.

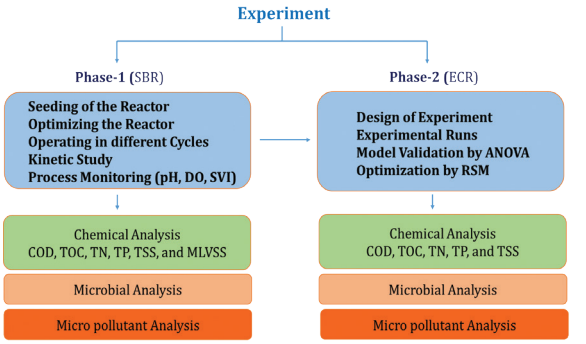

Figure 2: Flow diagram of the experimental procedure.

Phase-1

Seeding and operation of the SBR

The SBR was inoculated with the aeration tank sludge of an activated sludge process reactor, which was in operation for more than three years. A Mixed Liquor Suspended Solids (MLSS) of 5 g/L was achieved. After the start-up period, the SBR was operated at

four different cycles - 24, 16, 12, and 8 h. Each cycle consists of 5 phases: fill, aeration, settling, decant, and idle. The Dissolved Oxygen (DO) concentration in the reactor was kept within the range of 3–4 mg/L to maintain sufficient biomass in the reactor having good settling property.

Phase-2

Operation of ECR and process optimization

The ECR was connected in series when the SBR was operated at the 8-h cycle. Design of Experiment (DoE) was followed for process optimization. The coded and uncoded values and levels for the independent variables are shown in Table 1. The CCD design matrix is shown in Table 2. pH (X_1, 2–10), reaction time (X_2, 2–10 min), and current (X_3, 1–4 amp) were chosen as independent process variables. The removal of COD, DOC, TN, and TP was selected as dependent variables. Five-levels ($-\alpha$, –1, 0, +1 and $+\alpha$) were selected for the independent process variables. The CCD required a total of twenty experimental runs - eight factorial runs (2^k), six center points (n_c), and six axial points (2^k) [18], [19]. A second-order polynomial model, expressing the percentage removal as the function independent variables, was developed, as shown in Equation (6).

$$Y = \beta_D + \sum_{i=1}^{3} \beta_i X_i + \sum_{i=1}^{3} \beta_{ii} X_i^2 + \sum_{i=1}^{3} \sum_{j=i+1}^{3} \beta_{ij} X_i X_j \qquad (6)$$

Where Y is the predicted response for independent variables X_i, X_j, the constants in the equation β_0, β_i, β_{ii}, β_{ij} are constant-coefficient, ith linear coefficient, quadratic coefficient, and interaction coefficient, respectively. The data processing and optimization were performed using Design Expert 11.1.2.0 software.

Table 1: Coded and the uncoded values, and the levels of the independent variables

Independent Variable	Coded Terms	Coded Values				
		$-\alpha$	–1	0	+1	$+\alpha$
pH (X_1)	X_1	2.0	3.6	6.0	8.4	10
R Time (X_2, Min)	X_2	2.0	3.6	6.0	8.4	10
Current (X_3, Amp)	X_3	1	1.60	2.5	3.4	4

Table 2: CCD design matrix

RUN	Independent Variables			Response (Removal in %)			
	X_1	X_2	X_3	COD	DOC	TN	TP
1	3.6	3.6	1.6	54	65	63	92
2	8.4	3.6	1.6	47	55	48	72
3	3.6	3.6	3.4	67	74	59	96
4	8.4	3.6	3.4	70	72	40	95
5	3.6	8.4	1.6	75	76	48	97
6	8.4	8.4	1.6	60	68	26	94
7	3.6	8.4	3.4	67	78	63	75
8	8.4	8.4	3.4	67	70	49	94
9	2.0	6	2.5	60	53	67	74
10	10	6	2.5	60	48	48	74
11	6	6	1	65	69	29	96
12	6	6	4.0	77	80	43	98
13	6	2	2.5	51	69	59	96
14	6	10	2.5	67	82	53	100
15	6	6	2.5	78	80	50	97
16	6	6	2.5	78	74	43	99
17	6	6	2.5	83	80	45	97
18	6	6	2.5	75	78	38	96
19	6	6	2.5	75	76	39	97
20	6	6	2.5	83	80	45	97

2.4 *Analytical methods*

2.4.1 Physicochemical and organic constituent analysis

The pH, COD, DOC, TN, TP, TSS, and VSS were determined following the protocol given in the Standard Methods for the Examination of Water and Wastewater [20]. Total COD (CODt) was measured directly; for soluble COD (CODs) the samples were filtered through 0.45 µm pore size filters before digestion. DOC and TN contents were analyzed using the TOC-L analyzer (Make: Shimadzu, Model No. TOC-L analyzer, Hyderabad, India). A high-resolution accurate mass (HRAM) LC-MS/MS system (Agilent 6545 QTOF) was used for the analysis of the organic constituents. The details of the procedure for HRAM analysis are given elsewhere [21].

2.4.2 Sludge characterization

The sludge generated in SBR and ECR was characterized using Fourier Transform Infrared Spectroscopy (FTIR), X-ray diffraction (XRD), Scanning Electron Microscopy (SEM). XRD was performed with copper anticathode (Make: Rigaku, Model: Ultima IV). For

the phase identification, the diffractograms were explained using Xpert data collector software. FTIR analysis (Make: Jasco, Model: 4200) was performed to analyze the functional groups present in the samples. The sludge samples were scanned at a resolution of 4 cm^{-1} in the range of 4000–400 cm^{-1} wavenumber. SEM (Make: FEI, Model: Quanta FEG 250) shows the surface morphology of sludge at different magnifications. Before the analysis, the sludge samples were dried at 105°C temperature in the oven for two days.

3 Results and Discussion

3.1 *Phase-I*

3.1.1 Wastewater characteristics

The pH indicates that the inlet wastewater was slightly alkaline. The COD of the MWW was between 50,000 and 60,000 mg/L. However, during treatment in the existing anaerobic digester, almost 90% of COD was removed. The wastewater color was dark brown because of the presence of plant organic compounds. This anaerobically digested effluent was fed to the SBR followed by polishing in the ECR. The characteristics of the anaerobically digested effluent, which was fed to the SBR, are given in Table 3.

Table 3: Composition of MWW wastewater

Parameter	Average Value (Avg. Value)	Unit of Measurement
pH	8.33 ± 0.18	-
Color	Dark Brownish	-
COD	5750 ± 991	mg/L
DOC	980 ± 120	mg/L
BOD	2300 ± 50	mg/L
T-N	692 ± 60	mg/L
Nitrate-N	1.1 ± 0.3	mg/L
Total phosphorous	9.7 ± 1.1	mg/L
Suspended solids	1144 ± 166	mg/L

3.1.2 Process monitoring of the SBR

Temperature, pH, DO, MLSS, and Sludge Volume Index (SVI) level are important parameters that affect or indicate the growth and quality of microorganisms in bioreactors. The optimum temperature for aerobic biological treatment is between 25 and 35°C [11]. In this study, it was observed that the lowest temperature was 22.5°C and the highest temperature was 29.7°C. pH is another important factor that affects microbial growth. The pH range of 7.5–9.2 is good for the active growth of microorganisms [22]. In the present research, it was observed that the influent pH was 8.3 ± 0.18; the outlet pH was pH 8.61 ± 0.23, which was within the optimal range. A slight increase in pH was observed at the outlet, which was possibly due to the escape of carbon dioxide from the wastewater during the react phase due to the sparging effect of aeration.

DO is a critical factor for biological wastewater treatment [23]. Maintaining a DO concentration of 2 mg/L is essential for the activated sludge process; otherwise, it promotes the growth of filamentous bacteria and increases turbidity [11]. Low DO (0.5–2 mg/L) in the aeration tank results in activated sludge with poor settling properties. The thickening of sludge may also happen due to the accumulation of dead biomass. On the other hand, an excessively high DO level (> 5 mg/L) due to intense aeration may degrade the sludge quality by shearing of biomass and formation of bulkier sludge [24]. In this study, DO concentration was kept in the range of 2.5–3.5 mg/L to develop a good quality aerobic biomass with good settling properties.

Sludge settleability affects biological treatment efficiency and, therefore, is considered an important characteristic. SVI is the ratio of the percentage of the settled volume of sludge in 30 min to the percent by weight of MLSS in grams. SVI is one of the good indicators for assessing sludge stability in any aerobic activated sludge process. In this study, SVI was monitored after the end of the REACT phase of each cycle. An SVI of 150 mL/g is often considered the boundary between good settling sludge (SVI < 150) and poor settling sludge (SVI > 150) [22]. In this study, the average SVI was 67 mL/g, and sludge demonstrated good settling properties.

MLSS and Mixed Liquor Volatile Suspended Solids (MLVSS), which give an estimate of the concentration of microorganisms in a reactor, were monitored periodically. MLSS includes both inorganic and organic solids, while MLVSS indicates the concentration of organic solids, therefore, gives a better estimation of the microorganism concentrations [25]. Usually, the MLVSS is about 70% or 80% of MLSS in wastewater. The MLSS required for the effective functioning of the activated sludge process is 3000–6000 mg/L [11]. In this study, the MLSS and MLVSS of the reactor

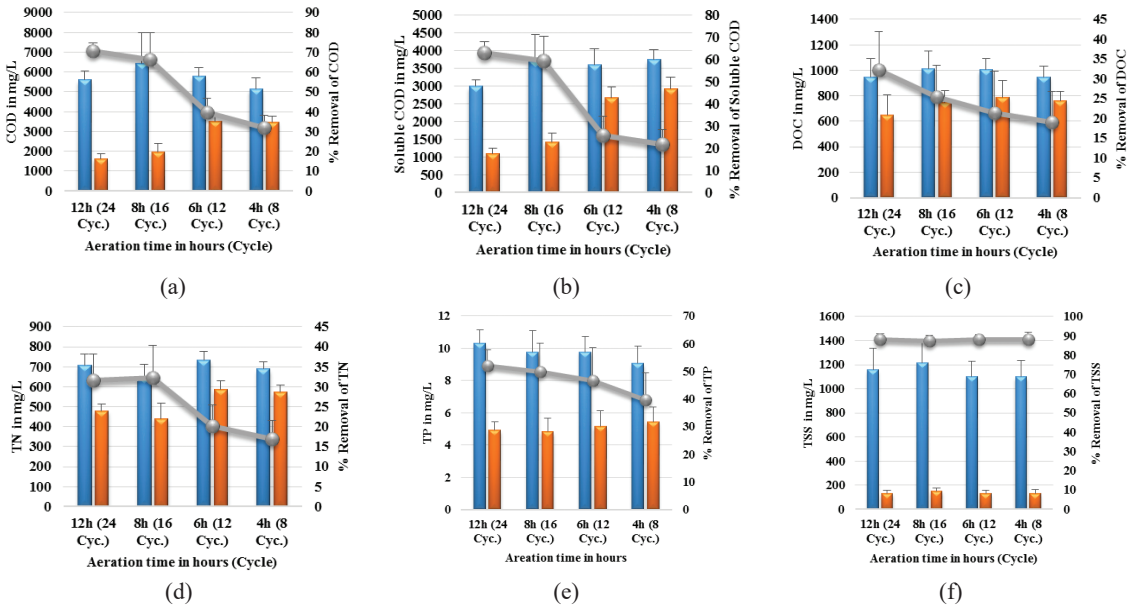

Figure 3: COD, DOC, TN removals at various HRTs of 12, 8, 6, and 4 h (a) Total COD removal (b) Soluble COD removal (c) DOC removal and (d) TN removal (e) TP removal (f) TSS removal.

varied from 5500–8000 mg/L and 2500–4000 mg/L, respectively. While treating high-strength wastewaters like anaerobically digested palm oil mill effluent, Fun [26] maintained an MLSS concentration of 2500–4000 mg/L. Popple [27] maintained an MLSS concentration of 3000 mg/L for investigating the fate of radioactively labeled pharmaceuticals. Bae [28] maintained MLSS of more than 8000 mg/L for the treatment of dairy industry wastewater.

3.1.3 Performance of the SBR

Figure 3 shows the COD, DOC, TN, TP, and TSS removal percentages for 24, 16, 12, and 8 h cycles. The total outlet COD was 1638 ± 231, 1977 ± 436, 3491 ± 303 and 3472 ± 301 mg/L for 24, 16, 12, and 8 h cycle, respectively; the corresponding removal efficiencies were 71, 66, 39, and 32%. The effluent dissolved COD was 1107 ± 147, 1432 ± 250, 2665 ± 305, and 2933 ± 320 mg/L for 24, 16, 12, and 8 h cycle, respectively, and the corresponding removal efficiencies were 63, 60, 26, and 22%. The effluent DOC was 646 ± 164, 750 ± 92, 790 ± 128, and 763 ± 74 mg/L which corresponds to 32, 26, 21, and 19% removal for 24, 16, 12, and 8 h cycle, respectively. The COD and DOC removal increased with the aeration time. Similar observations were reported in the literature as well [29].

Figure 3(d) represents the TN concentration and its removal at various cycles. TN removal efficiency was found to be around 32% at the 24 and 16 h cycles. However, TN removal at 12 and 8 h cycles dropped to 20 and 17%, respectively. The DO in the effluent ranged from 2.2 to 3.7 mg/L at all the cycles. It implies that assimilation and not denitrification was the dominant mechanism of nitrogen removal. Reduction of cycle time could have affected the assimilation of nitrogen in biomass; therefore, nitrogen in the supernatant at these two cycles was higher. The influent total phosphorus concentration was low, around 10 mg/L at all the cycles. The outlet concentrations were also around 5 mg/L, which implies that TP removal was similar at all the cycles. Figure 3(f) represents TSS concentration and its percentage removal at different cycles. As seen from the figure, the raw water TSS was between 1100 and 1200 mg/L. The average effluent TSS was below 150 mg/L at all the cycles. This corresponds to a removal efficiency of around 85%. Outlet TSS depends on the settling properties of sludge and the settling time.

The 'settle' phase was 3 h at all the cycles. During the SVI test, it was found that settling was completed within 60 min. Sufficient settling time was provided

during all the cycles.

3.2 *Phase-II*

3.2.1 Polishing treatment in ECR

The ECR was coupled with the SBR during an 8 h cycle to further bring down effluent COD, DOC, TN, and TP values. At the 8 h cycle of the SBR, the effluent COD was around 3500 mg/L and the treated effluent was still dark brown. It was decided to select this cycle to couple the ECR with the SBR and to operate the combined system at higher loading while further improving the quality of the treated effluent.

3.2.2 Design of experiment, model development & validation

CCD was used. A total of 20 experimental runs were performed in duplicates. The design matrix and the responses are shown in Table 2.

The significance and validity of the second-order models were determined by the Analysis of Variance (ANOVA). The significance of the quadratic models was determined using the coefficient of determination (R^2) value [30]. A coefficient of determination (R^2) value greater than 0.75 indicates that the model is significant [18]. In this work, the coefficient of determination for all the responses was greater than 0.90, which indicates satisfactory model performance. Further, adjusted R^2 values were used to check the model performance. As shown in Table 4, in all the cases, R^2, R^2-adjusted values were observed to be in close agreement with one another, demonstrating the significance of the model [30]. Therefore, the quadratic model was chosen for further analysis.

Table 4: Statistical parameters obtained from the analysis of variance for the quadratic models

Variables	COD Removal	DOC Removal	TN Removal	TP Removal
R^2	95.13%	94.85%	92.77%	99.67%
R^2 -adjusted	90.74%	90.21%	86.25%	99.38%

Table 5 represents the ANOVA results. It can be observed that P values of the model, linear, and quadratic terms for COD, DOC, TN, and TP removals were less than 0.05, which indicates that the quadratic model and terms were statistically significant, except for the 2-way interaction of DOC [31]. Moreover, the lack-of-fit values for all the cases were more than 0.05, which indicates that the model was statistically significant [9].

Table 5: ANOVA table

Source	DF	Adj SS	Adj MS	F-value	*p*-value
COD					
Model	9	1958.1	217.6	21.7	< 0.0001
Linear	3	482.6	160.9	16.0	< 0.0001
Square	3	1201.5	400.5	39.9	< 0.0001
2-Way Interaction	3	274.0	91.3	9.1	< 0.0001
Lack-of-Fit	5	29.5	5.9	0.4	0.821
DOC					
Model	9	1687.6	187.5	20.5	< 0.0001
Linear	3	432.6	144.2	15.7	< 0.0001
Square	3	1185.0	395.0	43.1	< 0.0001
2-Way Interaction	3	70.0	23.3	2.6	0.115
Lack-of-Fit	5	61.2	12.3	2.0	0.231
TN					
Model	9	2045.5	227.3	14.3	< 0.0001
Linear	3	1020.3	340.1	21.3	< 0.0001
Square	3	735.4	245.1	15.4	< 0.0001
2-Way Interaction	3	289.8	96.6	6.1	< 0.0001
Lack-of-Fit	5	61.7	12.3	0.6	0.7
TP					
Model	9	1715.4	190.6	338.6	< 0.0001
Linear	3	15.7	5.2	9.3	< 0.0001
Square	3	1007.6	335.9	596.6	< 0.0001
2-Way Interaction	3	692.1	230.7	409.9	< 0.0001
Lack-of-Fit	5	2.9	0.6	1.1	0.5

3.2.3 Significance of the process variables

The effects of three operating variables: initial pH (X_1), current (X_2), and reaction time (X_3) on COD, DOC, TN, and TP removals were investigated. Second-order quadratic equations (Equations 7–10) were fitted to the experimental data following multiple regression analysis. The regression models produced 3D surface plots, which have been explained individually. In the equations, the positive values of the coefficients indicate that the increase in main terms the efficiency of pollutant removal increase. All quadratic terms were observed with negative signs showing downward curvature in the surface plot. In interaction terms, the positive sign indicates that both variables jointly show a synergistic effect, while the negative sign designates that one variable positively affects while the other variable negatively affects the response [32].

Effect of variables on COD removal:

Equation 7 shows all the significant terms in the model

for COD removal.

$$Y_{COD} = -63.9 + 10.72\ pH + 24.97\ C + 23.41\ Time - 1.140\ pH*pH - 3.29\ C*C - 1.222\ Time*Time + 1.523\ pH*C - 0.239\ pH*Time - 2.210\ C*Time \quad (7)$$

The current was seen to be the most significant among the independent linear model terms and higher-order terms. The interaction between reaction time and the current was most significant among the interaction terms. The increase in pH, current, and time individually increased the COD removal. Figure 4(a) indicates the interaction of pH and current on COD removal. The COD removal efficiency peaked at around pH=6. The decrease in the removal efficiency was observed when pH was decreased below 4 or increased above 8. Similar results were reported in the EC treatment of anaerobically-treated municipal wastewater by [33]. Figure 4(b) represents the interaction of pH and reaction time on COD removal. The pattern of the graph indicates a plateau, which indicates that the highest COD removal could be achieved near the central values of the selected range of pH and reaction time.

In the EC operation, pH is an influencing factor in removing pollutants by converting Fe^{2+} ions to Fe^{3+} coagulants [13]. The surface charge of the coagulant can change with a change in pH. Charge neutralization and adsorption or indirect chemical oxidation are the possible mechanisms for DOC removal. When the pH is between 4 and 5.5, the charge neutralization dominates. Flocs of Fe $(OH)_3$ are observed when the range of pH is more than 7. These flocs accelerate the process of adsorption by providing more surface area [9]. When pH is less than 6, indirect chemical oxidation may happen that results in the escape of carbon in the form of carbon dioxide.

Figure 4(c) indicates the interaction between current and reaction time on COD removal, which shows improvement in removal efficiency with an increase in RT and current. The current plays an important role in the electrochemical processes. According to Faraday's law, with the increase in current and electrolysis time, the electrode dissolution increases from the anode. The active sites and surface area of the coagulant increase with a current, which helps in higher removal efficiency. However, after some time, a state of saturation is reached when the dissolution of anode decreases [31]. Consequently, removal also plateaus, as seen in Figure 4 (c).

Effect of variables on DOC removal:

The quadratic equation for DOC removal is represented by Equation (8) and explains all the important terms in the model for DOC removal.

$$Y_{DOC} = -12.2 + 17.60\ pH + 11.97\ C + 5.32\ Time - 1.593\ pH*pH - 0.55\ C*C + 0.004\ Time*Time + 0.424\ pH*C - 0.101\ pH*Time - 1.301 C*Time \quad (8)$$

The current was found to exert more effect on DOC removal among the independent linear model terms. The interaction between current and time was found to be the most significant among interaction terms. Chen [34] observed that the types of anions produced and the current influence the removal efficiency. Figure 4(d) represents the interaction of pH and current on DOC removal. The results reveal that around pH = 6, the DOC removal efficiency was maximum and removal efficiency increased with an increase in the current. Both COD and DOC removal rates were influenced by pH. Many studies reported that a pH of around 7.0 is optimum for treating different types of effluents in an EC process [35]. In the present study, the pH in the acidic region had shown good removal efficiency. Figure 4(e) indicates the interaction of pH and RT on DOC removal. It could be observed that with an increase in RT a moderate increase in DOC removal was noticed, whereas the removal reduced on either side of the optimal pH range. Figure 4(f) indicates the interaction of RT and current on DOC removal; the DOC removal efficiency increased with current but remained constant in the selected range of RT.

Effect of variables on TN removal:

The quadratic equation for TN removal is represented as Equation (9) and explains all the essential terms in the model for TN removal.

$$Y_{TN} = 139.7 - 13.76\ pH + 2.54\ C - 16.98\ Time + 0.860\ pH*pH - 3.36\ C*C + 0.764\ Time*Time + 0.228\ pH*C - 0.044\ pH*Time + 2.826\ C*Time \quad (9)$$

The reaction time effect among first-order coefficients and the current was showed more effect among second-order coefficients. The interaction between the reaction time and current had the highest

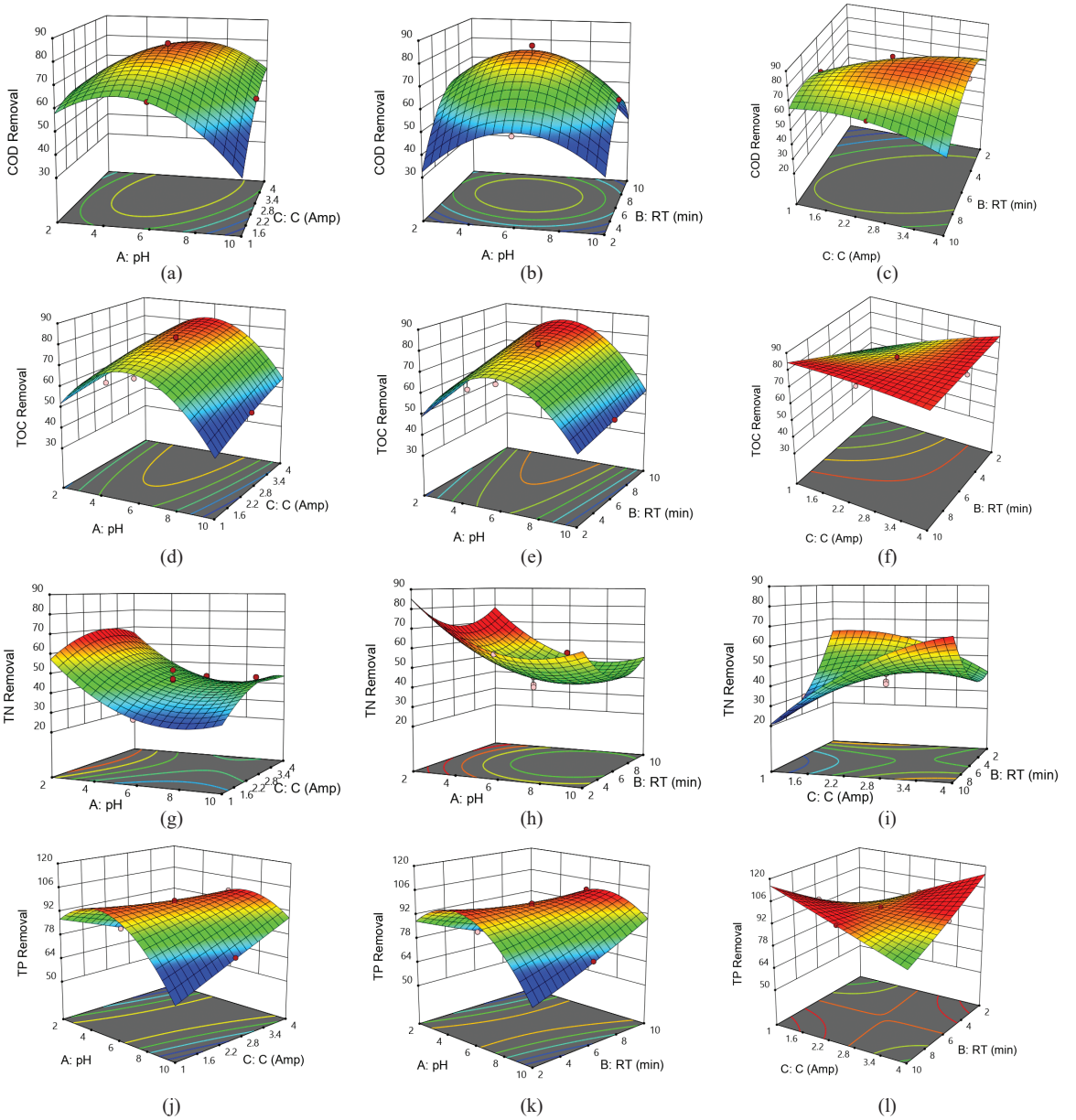

Figure 4: Response Surface plots for COD, DOC, TN and TP removal at different pH, current and reaction times. (a)–(c) COD (d)–(f) DOC (g)–(i) TN (j)–(l) TP.

effect on nitrogen removal among the interaction terms. Figure 4(g) represents the effect of the interaction between pH and current on TN removal. Similarly, Figure 4(h) shows the effect of interaction between pH and RT on TN removal. pH did not show any significant effect on nitrogen removal within the tested range (shown by the brown dots) although the model predicts higher removal at pH down to 2, which is practically not feasible to maintain in the system. As mentioned by Majlesi [36] nitrogen usually escapes from water in the form of N_2 gas or ammonia. Since adsorption or precipitation mechanisms do not play any dominant role in the removal of nitrogen, the effect of pH is negligible. On the other hand, the metal ions released

during the electrochemical process play a dominant role in reducing nitrate to N_2 gas and ammonia. As per Faraday's Law, the amount of metal ions released from the electrode depends on the current and the time of electrolysis. Therefore, the current and reaction time have more effect on nitrogen removal. However, if the current and/or the electrolysis time is increased indefinitely, a saturation may occur when the ions, already present in the solution, may hinder further release of ions, through the dissolution of the anode, therefore, a plateau in the removal graph may be seen as shown in Figure 4(i). That is why higher removal was not seen at the point corresponding to the highest current and reaction time. Rather, the model predicted higher removal (red region) when the reaction time was less and the current was more as well as when the current was more and the corresponding reaction time was less. Overall, the ECR was not very effective in removing nitrogen. The removals of the other parameters were higher as shown in Table 6.

Effect of variables on TP removal:

The quadratic equation for TP removal is represented as Equation (10) and explains all the important terms in the model for TP removal.

$$Y_{TP} = 67.37 + 6.225\ pH + 4.25\ C + 1.504\ Time - 1.4576\ pH*pH - 0.097\ C*C + 0.0722\ Time*Time + 2.368\ pH*C + 0.8629\ pH*Time - 2.885\ C*Time \quad (10)$$

pH was observed to be a significant parameter among the first and the second-order terms. The interaction between current and RT appeared to have exerted more influence on the removal of TP.

Figure 4(j) represents the interaction of pH and current and Figure 4(k) represents the interaction of pH and RT on TP removal. The ridge pattern was observed in both the figures which means only one of the two interacting parameters dominated. The efficiency of TP removal was in the region of maxima when the pH was around 6. pH was the dominating factor in both cases. It was observed that the ECR worked best at the neutral pH. Adsorption and chemical precipitation are the two methods by which TP is removed. Both mechanisms are pH-dependent. Again, the model predicted higher TP removals (red region) when the current was high and the corresponding reaction time was low, and also when the reaction time was high and the corresponding current was low. As mentioned in the previous section, these are the regions where the availability of metal ions is high.

3.2.4 Multi-objective optimization

Multiple response optimization can be performed by using the Response Surface Methodology. It converts multiple responses into a single one by combining individual responses into a composite function followed by its optimization [37]. The desirability function-based approach consists of converting each response into individual desirability functions (d) that are then aggregated into a composite function (D), which is usually geometric or arithmetic mean [33]. Each response process variable is transformed into a dimensionless desirability scale 0–1 range. The d = 0 indicates undesirable response, d = 1 indicates the desired response and the composite desirability function D is the weighted geometric average of the responses [38]. In this study, the responses considered for optimization were COD removal efficiency, DOC removal efficiency, TN removal efficiency, and TP removal efficiency. The maximum and the minimum values in the CCD table (Table 1) were chosen to be the upper and the lower bounds. All four responses were given the same weight. The optimum condition obtained in this study was pH: 5.40, Current: 3.34 amp, and time: 4.56 min with composite desirability of 0.78. For model validation, an experimental run was performed at the optimum condition in triplicate. The sample from the optimized experimental run was used to find the responses and compared them with the predicted responses from the model.

A comparison between the experimental and model values is shown in Table 6. The COD, DOC, TN, and TP removals were observed to be 70%, 77.42%, 43.92%, and 97.68%, respectively. There was a good agreement between observed and predicted responses at the optimized points.

Table 6: Comparison between the experimental and model values

	% COD Removal	% DOC Removal	% TN Removal	% TP Removal
Model Value	76.73	79.91	45.94	99.90
Exp. Value	70.00	77.42	43.92	97.68

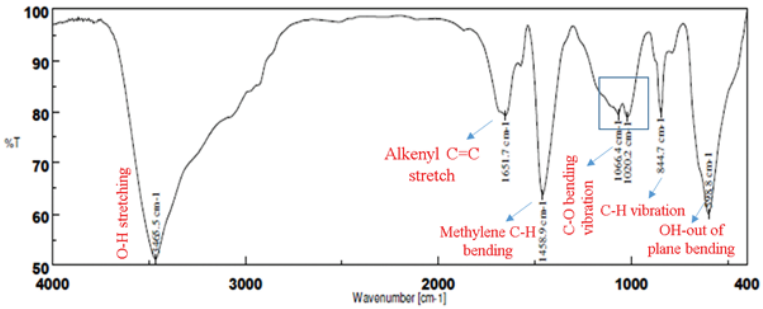

(a)

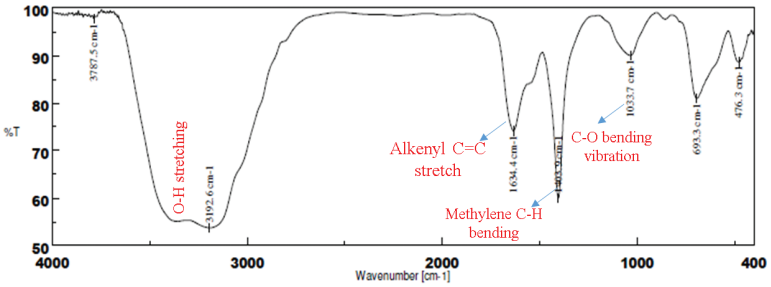

(b)

Figure 5: FTIR spectrum (a) SBR sludge (b) ECR sludge.

In one of the earlier studies, the ECR was used to polish the MWW after a sequential anaerobic-ASP (Activated Sludge Process) treatment. The DOC and TP removal efficiencies were 65% and 67%, respectively [9]. As seen in Table 6, the performance of the ECR enhanced significantly after ASP was replaced by SBR.

Sludge characterization:

Sludge management is a major problem in wastewater treatment systems. The characterization of the sludge helps in proposing suitable management techniques, including possible resource recovery and other useful applications, and explaining the mechanism of pollutant removal. In the present study, the SBR sludge and ECR sludge were collected and oven-dried at 105°C for 24 h. The dried sludge samples from the two reactors were characterized using XRD and FTIR analysis.

The FTIR spectrum of the SBR sludge and ECR sludge have been shown in Figure 5. From the figure, it can be observed that there were changes in the positions of functional groups in both spectra. The change in the peaks toward lower wavenumbers from higher wavenumbers is due to a reduction in the molecule mass [39]. In the SBR sludge, the major peaks at 3465, 1651, 1458, 598 were due to OH-stretching, alkenyl C-C stretching, methylene C-H bending, and O-H out of plane bending, respectively. The shallow broad peaks in the wavelength range of 1150–950 cm^{-1} indicate the C-O bending vibrations in carbohydrates present in the sludge sample [40]. However, the reduction and the disappearance of peaks in the same region in ECR sludge indicate the removal of organic matter during electrocoagulation. The transmittance peak at 844 cm^{-1} in SBR, indicates the vibrations in the anomeric region of carbohydrates (C–H deformation), which completely disappeared after electrocoagulation [41]. In the FTIR spectrum of ECR sludge, the broad peak in the range of 3500–3000 cm^{-1} was due to the presence of hydrogen-bonded O-H stretching of iron oxy-hydroxides [42]. This broadened peak in the ECR sludge confirms the formation of ferrous ion flocs during the electrocoagulation process. The sharp peak at 693 cm^{-1} was due to the presence of magnetite (Fe_3O_4) and the shallow transmittance peak at 476 cm^{-1} indicates the existence of ferrous oxide (FeO) [43]. This presence of iron oxy-hydroxide peaks in the ECR sludge indicates oxygen evolution during the electrocoagulation process which also facilitates indirect chemical oxidation of organic matter [9].

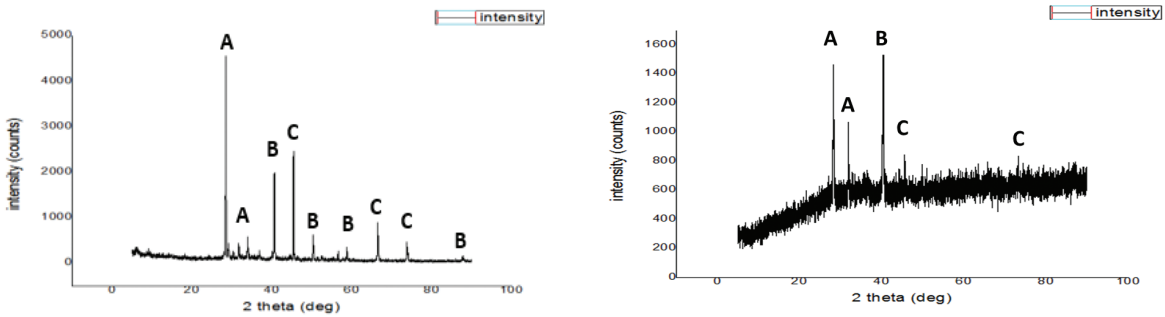

(a) (b)

Note: (A)- JCPDS-44-0782; (B)- JCPDS-17-0837; (C)- JCPDS-89-6096

Figure 6: XRD pattern of (a) SBR sludge (b) ECR sludge.

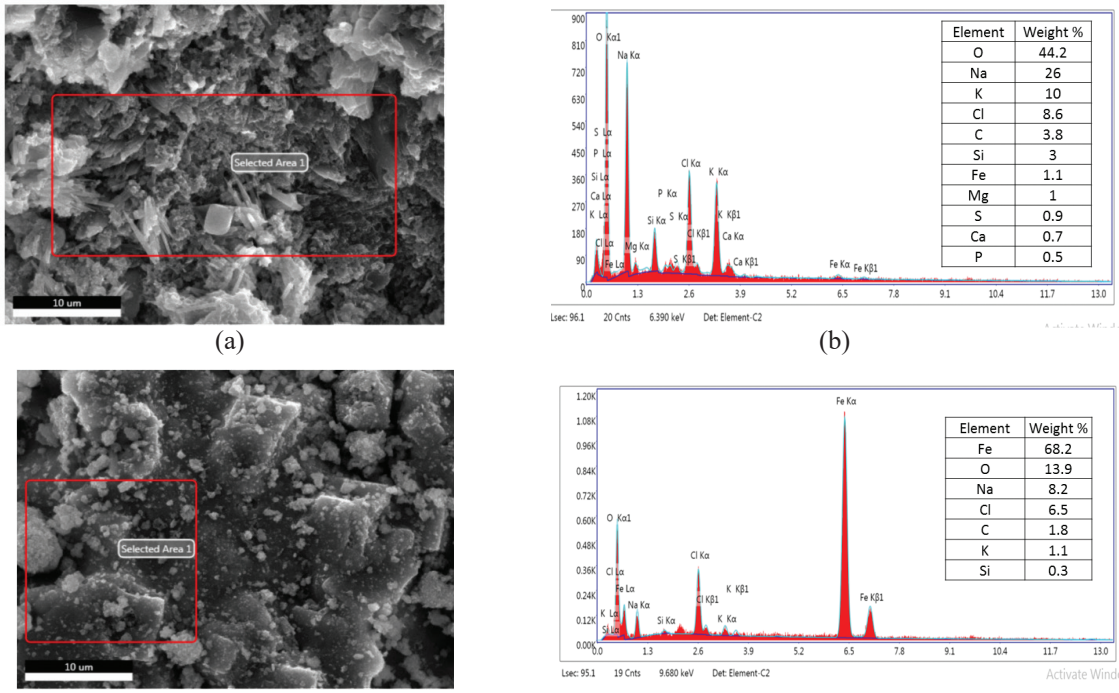

(a) (b)

(c) (d)

Figure 7: SEM-EDX images of (a-b) SBR sludge (c-d) ECR sludge.

To understand the mechanism involved in the process of removal of pollutants XRD analysis was done. The presence of compounds such as phosphoric acid (H_3PO_4), iron hydroxide ($Fe(OH)_3$) indicates the adsorption mechanism, and the presence of iron phosphate ($FePO_4$) indicates the precipitation mechanism. Based on peak positions observed in Figure 6(a), denotes the presence of H_3PO_4 at point A (JCPDS-44-0782), $FePO_4$ at point B (JCPDS-17-0837), and $Fe(OH)_3$ at point C (JCPDS-89-6096). In SBR, the presence of H_3PO_4 and $Fe(OH)_3$ as major peaks and $FePO_4$ as a minute peak indicates that the adsorption mechanism is prominent. In ECR, the presence of phosphoric acid and $FePO_4$ as major peaks indicates chemical precipitation is a prominent mechanism.

Sludge after SBR and ECR were observed using a Scanning electron microscope (SEM) coupled with an Energy Dispersion Spectroscopy (EDS). Figure 7(a)

and (b) show the surface morphology of SBR and ECR. It is clear from the SEM images that the SBR and ECR samples exhibited particles with random size and shape. As seen in figure, the elemental analysis of SBR and ECR sludge by EDS showed elements in the following order as per weight percent (%): O >Na >K >Cl >C >Si >Fe >Mg > S > Ca > P (0.6) and Fe > O > Na > Cl >C > K > Si, respectively. The sludge characteristics would depend upon the wastewater characteristics being treated and the type of electrode being used [44]. When the image before and after ECR treatment was compared, some of the elements disappeared and some decreased drastically. However, the iron content increased from 1.1 (SBR sludge) to 68.2 (in ECR sludge), which was due to the use of iron electrodes.

3.3 *Analysis of the organic constituents*

The LC-HRMS analysis was carried out to identify the organic compounds in the inlet and the treated wastewater and their removal. The removal percentages were calculated based on the abundance values (area under the peak in the mass spec) of the compounds at the inlet and the outlet. Table 7 lists the organic compounds and their removals. Natural plant compounds, synthetic plant hormones, metabolites, and pesticides were found in the wastewater. For a good yield of the crop, farmers generally apply fertilizers, growth hormones, and pesticides. While some of these organic constituents are biodegradable, several such compounds are bio-refractory, therefore, difficult to remove in a standalone biological system. Therefore, a biological treatment followed by physicochemical polishing can provide better removal. As seen from the table, SBR ensured significant removal of all the identified components, while SBR-ECR coupled system was capable of removing almost all the constituents that were identified.

The electrochemical reaction results in the in-situ formation of coagulant in water due to oxidation of a sacrificial anode. Metal complexes, for example, (Fe(OH)n[s]), react with the pollutants in the wastewater causing adsorption of dissolved organic compounds [13]. In addition to adsorption, chemical oxidation at the electrode helps in a significant reduction of DOC. The high molecular weight fraction of the organic compounds is also degraded into lesser molecular weight compounds having hydrophilic nature. Ensano [15] found electrocoagulation is an effective method for degrading refractory pharmaceutical active compounds.

The outlet water characteristics and discharge criteria for inland surface water and land irrigation, set by the regulatory body of India [45], are given in Table 8.

Table 7: Removal of organic constituents

Name of the Compound	Type of Compound	SBR Inlet Abundance	SBR Outlet Abundance	ECR Outlet Abundance	% Rem SBR OT	% Rem ECR OT
Hinokitiol	Plant compound	88535	17815	0	80	100
Ionone	Contributor for the aroma	88698	10169	8029	89	91
Trinexapac-ethyl	Plant growth regulator	149469	55237	0	63	100
Ethyl 4-hydroxy benzoate	Plant metabolite	532403	12644	0	98	100
Salicylic acid	Plant growth regulator	38001	0	0	100	100
Methylsalicylate	Plant hormone that fight against disease	74882	16976	0	77	100
(Â±)-Limonene	Found in the peels of fruits	120022	9499	0	92	100
Heptylparaben	Agricultural chemical	48033	20175	0	58	100
2-Pentylphenol	Fungicide	166273	10905	0	93	100
Aniline	Fungacide and herbicide	41230	7798	0	81	100
Cyprodinil	Agricultural fungicide	47966	20726	0	57	100
Diphenylamine	Fungicide and antihelmintic	279217	104896	0	62	100
NButylbenzenesulphonamide	Antifungal properties	192591	16864	0	91	100
Pyroquilon	Antifungal agrochemical	77349	28087	0	64	100
Carbetamide	Carbamate herbicide	27637	11359	0	59	100
Atrazine-desethyl	Herbicide	77794	14767	0	81	100
Bendiocarb	Carbamate insecticide	76111	22168	0	71	100
2,6-di-tert-butyl-p-Cresol (BHT)	Used in pesticide formulations	253667	13596	0	95	100

Table 8: Outlet wastewater characteristics (average values) after SBR (8 h cycle) and ECR treatment

Parameter	SBR Inlet (mg/L)	SBR Outlet (mg/L)	ECR Outlet (mg/L)	% Removal after SBR	% Removal after ECR	% Overall removal	Standards for Inland Surface Water (mg/L)[a]	Standards for Land for Irrigation (mg/L)[a]
BOD	2300	1650	333	28	80	86	30	100
COD	5200	3600	1080	31	70	79	250	-
TN	668	562	315	16	44	53	100	-
TP	9.1	5.4	0.12	40	98	99	-	-
TSS	1102	129	0.00	88	100	100	100	200
VSS	120	42	0.00	65	100	100	-	-
pH (unit less)	8.2	8.5	8.71	-	-	-	5.5–9.0	5.5–9.0

Note: ([a])- CPCB, (2015); (--) Not available

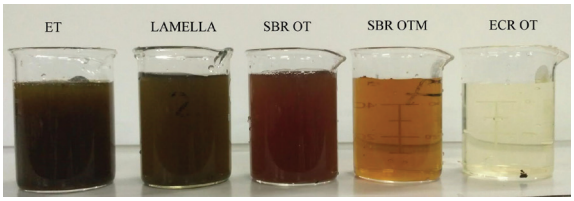

Figure 8: Color of the wastewater in the Equalization tank, after Lamella Clarifier (after anaerobic digestion), at SBR Outlet and ECR outlet, respectively.

For irrigation, no limit on COD has been placed but the BOD and TSS should be below 100 mg/L and 200 mg/L, respectively, while pH should be between 5.5–9. For discharge to inland surface water, the criteria are stricter. The present setup was able to bring the COD down to 1080 mg/L from an initial value of 5200 mg/L. TSS was completely removed and pH was also within the range. However, outlet BOD was around 333 mg/L which was more than the discharge limit for land application (100 mg/L). As seen in Figure 8, the outlet sample from the ECR was very clean. Therefore, a tertiary advanced oxidation process is recommended. Such a process would oxidize the organic carbon from the treated water while preserving its nutrient content so that the final effluent can be used in irrigation.

4 Conclusions

SBR performance was good at 24, 16, 12, and 8 h cycles. However, the performance decreased with a decrease in the cycle time. An ECR was integrated with the SBR operated in an 8-h cycle to bring down the effluent COD, DOC, TN, and TP values further. The SBR-ECR combination was able to significantly reduce the time of treatment. COD, DOC, TN, and TP removal were observed to be 79, 85, 53, and 99%, respectively when the SBR was operated at an 8 h cycle and the ECR was operated at 4.57 min. The color was removed. Suspended solids were also reduced to a level below the detection limit. The final effluent still contains an appreciable amount of COD, in dissolved form. The effluent did not show any presence of pathogenic bacteria; as the wastewater is generated from a food processing plant and, therefore, may be reused for irrigating non-food crops. But BOD has to be brought down further to meet the discharge limit for irrigation. An advanced oxidation process may be used that will reduce the organic carbon but the nutrient level will not be altered. However, to use the treated water for industrial or other non-potable purposes even the nutrient level needs to be brought down. In that case, RO is the only option.

Acknowledgments

The authors gratefully acknowledge the financial support received from the Ministry of Human Resource Development of India, Science and Engineering Research Board of India, and Rahyals Envergy India Pvt Ltd through the research initiative Uchchatar Avishkar Yojana. Besides, the authors would like to thank Synthite Industries Pvt Ltd. for providing space and other on-site facilities for this research and extend thanks to Mr. Prashanth of Agilent Technologies for his support in the organic constituent analysis.

References

[1] R. Rajagopal, N. M. C. Saady, M. Torrijos, J. V. Thanikal, and Y. T. Hung, “Sustainable agro-food

industrial wastewater treatment using high rate anaerobic process," *Water (Switzerland)*, vol. 5, no. 1, pp. 292–311, 2013, doi: 10.3390/w5010292.

[2] S. K. Pattanayak, *State of Indian Agriculture (2015–16)*. New Delhi, India: Government of India, 2017.

[3] K. Jayathilakan, K. Sultana, K. Radhakrishna, and A. S. Bawa, "Utilization of byproducts and waste materials from meat, poultry and fish processing industries: A review," *Journal of Food Science and Technology*, vol. 49, no. 3, pp. 278–293, 2012, doi: 10.1007/s13197-011-0290-7.

[4] E. Alayu and Z. Yirgu, "Advanced technologies for the treatment of wastewaters from agro-processing industries and cogeneration of by-products: A case of slaughterhouse, dairy and beverage industries," *International Journal of Environmental Science and Technology*, vol. 15, no. 7, pp. 1581–1596, 2018, doi: 10.1007/s13762-017-1522-9.

[5] W. Riansa-ngawong, W. Savedboworn, and M. Suwansaard, "Optimization of hydrogen production from pickle bamboo shoot wastewater by rhodopseudomonas palustris TN1," *King Mongkut's University of Technology North Bangkok International Journal of Applied Science and Technology*, vol. 8, no. 3, pp. 1–8, 2015, doi: 10.14416/j.ijast.2015.06.004.

[6] M. Wang, R. Tsao, S. Zhang, Z. Dong, R. Yang, J. Gong, and Y. Pei, "Antioxidant activity, mutagenicity/anti-mutagenicity, and clastogenicity/anti-clastogenicity of lutein from marigold flowers," *Food and Chemical Toxicology*, vol. 44, no. 9, pp. 1522–1529, 2006, doi: 10.1016/j.fct.2006.04.005.

[7] A. Tawai, K. Kitsubthawee, C. Panjapornpon, and W. Shao, "Hybrid control scheme for anaerobic digestion in a CSTR-UASB reactor system," *Applied Science and Engineering Progress*, vol. 13, no. 3, pp. 213–223, 2020, doi: 10.14416/j.asep.2020.06.004.

[8] H. Liu, Y. Wang, C. Liang, Q. Yang, S. Wang, B. Wang, F. Zhang, L. Zhang, H. Cheng, S. Song, and Liping Zhang, "Utilization of marigold (Tagetes erecta) flower fermentation wastewater as a fertilizer and its effect on microbial community structure in maize rhizosphere and non-rhizosphere soil," *Biotechnology & Biotechnological Equipment*, vol. 34, no. 1, pp. 522–531, 2020, doi: 10.1080/13102818.2020.1781548.

[9] M. Damaraju, D. Bhattacharyya, T. K. Panda, and K. K. Kurilla, "Marigold wastewater treatment in a lab-scale and a field-scale continuous bipolar-mode electrocoagulation system," *Journal of Cleaner Production*, vol. 245, p. 118693, 2020, doi: 10.1016/j.jclepro.2019.118693.

[10] M. Damaraju, V. K. Gupta, D. Bhattacharyya, T. K. Panda, and K. K. Kurilla, "Improving the performance of a continuous bipolar-mode electrocoagulation (CBME) system, treating a marigold flower processing wastewater, through process modifications," *Separation Science and Technology*, vol. 56, no. 3, pp. 1–13, 2021, doi: 10.1080/01496395.2020.1725572.

[11] W. Metcalf and C. Eddy, *Metcalf and Eddy Wastewater Engineering: Treatment and Reuse*. New York: McGraw Hill, 2003.

[12] P. G. Patil, G. S. Kulkarni, S. S. V Kore, and S. V. S. Kore, "Aerobic sequencing batch reactor for wastewater treatment: A review," *International Journal of Engineering Research and Technology*, vol. 2, no. 10, pp. 534–550, 2013.

[13] B. K. Zaied, M. Rashid, M. Nasrullah, A. W. Zularisam, D. Pant, and L. Singh, "A comprehensive review on contaminants removal from pharmaceutical wastewater by electrocoagulation process," *Science of the Total Environment*, vol. 726, p. 138095, 2020, doi: 10.1016/j.scitotenv.2020.138095.

[14] M. Damaraju, D. Bhattacharyya, T. K. Panda, and K. K. Kurilla, "Downstream processing of palm oil mill effluent in a CBME reactor," *Journal of Hazardous, Toxic, and Radioactive Waste*, vol. 24, no. 1, pp. 1–10, 2020, doi: 10.1061/(ASCE)HZ.2153-5515.0000484.

[15] B. M. B. Ensano, L. Borea, V. Naddeo, V. Belgiorno, M. D. G. de Luna, and F. C. Ballesteros, "Removal of pharmaceuticals from wastewater by intermittent electrocoagulation," *Water (Switzerland)*, vol. 9, no. 2, pp. 1–15, 2017, doi: 10.3390/w9020085.

[16] B. M. B. Ensano, L. Borea, V. Naddeo, V. Belgiorno, M. D. G. de Luna, M. Balakrishnan, and F. C. Ballesteros Jr, "Applicability of the electrocoagulation process in treating real municipal wastewater containing pharmaceutical active compounds," *Journal of Hazardous Materials*, vol. 361, pp. 367–373, 2019, doi:

10.1016/j.jhazmat.2018.07.093.

[17] J. Heffron, D. R. Ryan, and B. K. Mayer, "Sequential electrocoagulation-electrooxidation for virus mitigation in drinking water," *Water Research*, vol. 160, pp. 435–444, 2019, doi: 10.1016/j.watres.2019.05.078.

[18] W. Subramonian, T. Y. Wu, and S. Chai, "An application of response surface methodology for optimizing coagulation process of raw industrial effluent using Cassia obtusifolia seed gum together with alum," *Industrial Crops and Products*, vol. 70, pp. 107–115, 2015, doi: 10.1016/j.indcrop.2015.02.026.

[19] D. Montgomery, *Design and Analysis of Experiments*. 7th ed., New York: John Wiley and Sons, 2008.

[20] APHA, *Standard Methods for the Examination of Water and Wastewater*. 23rd ed., Washington, DC: APHA, 2012.

[21] L. K. Akula, V. B. Gaddam, M. Damaraju, D. Bhattacharyya, and K. K. Kurilla, "Domestic wastewater treatment in a coupled sequential batch reactor-electrochemical reactor process," *Water Environment Research*, pp. 1–3, 2020, doi: 10.1002/wer.1488.

[22] C. P. L. Grady, G. T. Daigger, N. G. Love, and C. D. M. Filipe, *Biological Wastewater Treatment*. 3rd ed., Florida: CRC Press, 2011.

[23] W. Jia , S. Liang, H. H. Ngo, W. Guo, J. Zhang, R. Wang, and Y. Zou, "Effect of phosphorus load on nutrients removal and N_2O emission during low-oxygen simultaneous nitrification and denitrification process," *Bioresource Technology*, vol. 141, pp. 123–130, 2013, doi: 10.1016/j.biortech.2013.02.095.

[24] G. Harja, I. Nascu, C. Muresan, and I. Nascu, "Improvements in dissolved oxygen control of an activated sludge wastewater treatment process," *Circuits, Systems, and Signal Processing*, vol. 35, no. 6, pp. 2259–2281, 2016, doi: 10.1007/s00034-016-0282-y.

[25] Y. J. Chan, M. F. Chong, and C. L. Law, "Biological treatment of anaerobically digested palm oil mill ef fl uent (POME) using a lab-scale sequencing batch reactor (SBR)," *Journal of Environmental Management*, vol. 91, no. 8, pp. 17381746, 2010, doi: 10.1016/j.jenvman.2010.03.021.

[26] C. W. Fun, M. R. U. Haq, and S. R. M. Kutty, "Treatment of palm oil mill effluent using biological sequencing batch reactor system," *WIT Transactions on Ecology and the Environment*, vol. 104, pp. 511–518, 2007, doi: 10.2495/RM070481.

[27] T. Popple, J. B. Williams, E. May, G. A. Mills, and R. Oliver, "Evaluation of a sequencing batch reactor sewage treatment rig for investigating the fate of radioactively labelled pharmaceuticals: Case study of propranolol," *Water Research*, vol. 88, pp. 83–92, Jan. 2016, doi: 10.1016/j.watres.2015.09.033.

[28] T. H. Bae, S. S. Han, and T. M. Tak, "Membrane sequencing batch reactor system for the treatment of dairy industry wastewater," *Process Biochemistry*, vol. 39, no. 2, pp. 221–231, Oct. 2003, doi: 10.1016/S0032-9592(03)00063-3.

[29] B. Kayranli and A. Ugurlu, "Effects of temperature and biomass concentration on the performance of anaerobic sequencing batch reactor treating low strength wastewater," *Desalination*, vol. 278, no. 1–3, pp. 77–83, Sep. 2011, doi: 10.1016/j.desal.2011.05.011.

[30] M. V. Jadhav and Y. S. Mahajan, "Application of response surface methodology to water/wastewater treatment using Coccinia indica," *Desalination and Water Treatment*, vol. 52, no. 34–3, pp. 37–41, 2014, doi: 10.1080/19443994.2013.821043.

[31] M. Kumar, F. I. A. Ponselvan, J. R. Malviya, V. C. Srivastava, and I. D. Mall, "Treatment of bio-digester effluent by electrocoagulation using iron electrodes," *Journal of Hazardous Materials*, vol. 165, no. 1–3, pp. 345–352, 2009, doi: 10.1016/j.jhazmat.2008.10.041.

[32] T. Shojaeimehr, F. Rahimpour, and M. Ali, "A modeling study by response surface methodology (RSM) and artificial neural network (ANN) on Cu 2^+ adsorption optimization using light expended clay aggregate (LECA)," *Journal of Industrial and Engineering Chemistry*, vol. 20, no. 3, pp. 870–880, 2014, doi: 10.1016/j.jiec.2013.06.017.

[33] A. R. Makwana and M. M. Ahammed, "Continuous electrocoagulation process for the post-treatment of anaerobically treated municipal wastewater," *Process Safety and Environmental Protection*, vol. 102, pp. 724–733, Jul. 2016, doi: 10.1016/j.psep.2016.06.005.

[34] G. Chen, "Electrochemical technologies in

wastewater treatment," *Separation and Purification Technology*, vol. 38, no. 1, pp. 11–41, 2004, doi: 10.1016/j.seppur.2003.10.006.

[35] S. Garcia-Segura, M. M. S. G. Eiband, J. V. de Melo, and C. A. Martínez-Huitle, "Electrocoagulation and advanced electrocoagulation processes: A general review about the fundamentals, emerging applications and its association with other technologies," *Journal of Electroanalytical Chemistry*, vol. 801, pp. 267–299, 2017, doi: 10.1016/j.jelechem.2017.07.047.

[36] M. Majlesi, S. M. Mohseny, M. Sardar, S. Golmohammadi, and A. Sheikhmohammadi, "Improvement of aqueous nitrate removal by using continuous electrocoagulation/electroflotation unit with vertical monopolar electrodes," *Sustainable Environment Research*, vol. 26, no. 6, pp. 287–290, 2016, doi: 10.1016/j.serj.2016.09.002.

[37] N. R. Costa, J. Lourenço, and Z. L. Pereira, "Desirability function approach: A review and performance evaluation in adverse conditions," *Chemometrics and Intelligent Laboratory Systems*, vol. 107, no. 2, pp. 234–244, 2011, doi: 10.1016/j.chemolab.2011.04.004.

[38] M. A. Bezrra, R. Erthal, E. Padua, L. Silveira, and L. Am, "Response surface methodology (RSM) as a tool for optimization in analytical chemistry," *Talanta*, vol. 76, no. 5, pp. 965–977, 2008, doi: 10.1016/j.talanta.2008.05.019.

[39] K. Gautam, S. Kamsonlian, and S. Kumar, "Removal of Reactive Red 120 dye from wastewater using electrocoagulation: optimization using multivariate approach, economic analysis, and sludge characterization," *Separation Science and Technology*, vol. 55, no. 18, pp. 3412–3426, 2020, doi: 10.1080/01496395.2019.1677713.

[40] J. Coates, "Interpretation of infrared spectra, a practical approach," *Encyclopedia of Analytical Chemistry*, pp. 1–23, 2006, doi: 10.1002/9780470027318.a5606.

[41] M. Kędzierska-Matysek, A. Matwijczuk, M. Florek, J. Barłowska, A. Wolanciuk, A. Matwijczuk, E. Chruściel, R. Walkowiak, D. Karcz, and B. Gładyszewska, "Application of FTIR spectroscopy for analysis of the quality of honey," *BIO Web of Conferences*, vol. 10, p. 02008, 2018, doi: 10.1051/bioconf/20181002008.

[42] Z. B. Gönder, G. Balcıoğlu, I. Vergili, and Y. Kaya, "Electrochemical treatment of carwash wastewater using Fe and Al electrode: Techno-economic analysis and sludge characterization," *Journal of Environmental Management*, vol. 200, pp. 380–390, 2017, doi: 10.1016/j.jenvman.2017.06.005.

[43] J. A. Gomes, P. Daida, M. Kesmez, M. Weir, H. Moreno , J. R. Parga, G. Irwin, H. McWhinney, T. Grady, E. Peterson, and D. L. Cocke, "Arsenic removal by electrocoagulation using combined Al-Fe electrode system and characterization of products," *Journal of Hazardous Materials*, vol. 139, no. 2, pp. 220–231, 2007, doi: 10.1016/j.jhazmat.2005.11.108.

[44] M. Kobya, F. Ulu, U. Gebologlu, E. Demirbas, and M. S. Oncel, "Treatment of potable water containing low concentration of arsenic with electrocoagulation: Different connection modes and Fe-Al electrodes," *Separation and Purification Technology*, vol. 77, no. 3, pp. 283–293, 2011, doi: 10.1016/j.seppur.2010.12.018.

[45] Central Pollution Control Board (CPCB), *Pollution Control Acts, Rules and Notification There*. Delhi, India: Central Pollution Control Board, 2015.